32nd Annual International Conference of the IEEE EMBS
Buenos Aires, Argentina, August 31 - September 4, 2010

Respiration effect on single and multi lead ECG delineation strategies

M. Noriega, J.P. Martínez, P. Laguna, D. Romero, R. Bailón and R. Almeida

Abstract—The main purpose of this work is to study the influence of the mechanical effect of the respiration over T wave end delineation. The performance of automatic delineation systems based in Wavelet Transform (WT) was compared, considering single lead (SL), post processing selection rules (SLR) and multi lead (ML) approaches. The T wave locations obtained over real and simulated ECG signals were analyzed together with the respective respiratory signal (ECG-derived or simulated). The linear relation between the variations on obtained marks and the mechanical effect of the respiration was measured using spectral coherence. With respect to the ML strategy we also explored the evolution of the vectorcardiographic spatial loop using the direction of maximum projection of the WT in the region close to the T wave end (T_e). The relation between this direction and the respiration is also explored.
The marks obtained from the SLR and ML delineation strategies show advantage over the SL strategy based marks. The coherence around the respiratory frequency between the respiratory signal and the error in T end marks was found to be higher using SLR (a minimum of 0.92) than using ML (a maximum of 0.80). According to obtained results, the multi lead delineation presents a lower sensibility to the mechanical effect of the respiration for the T wave end delineation, particularly the obtained with ML.

I. Introduction

Each heart beat is produced by an electric wavefront that crosses the different cardiac structures; the activation/inactivation of those correspond to different waves in the electrocardiogram (ECG) (Fig. 1). By using several electrodes it is possible to access simultaneous *electrocardiographic leads*, providing a spacial perspective [1]. The cardiac dipole model approximates the electrical activity from the heart by an time-variant electrical dipole called electric heart vector (EHV) [2]. In this model each lead can be interpreted as the projection of EHV on the vector that defines the lead direction. The EHV's canonical representation is given by the vectorcardiogram (VCG) defined by 3 orthogonal leads $[x(n), y(n), z(n)]$, usually acquired as the corrected Frank leads.

M. Noriega and D. Romero are with the *Comunications and Electronical Departament of Oriente University*, Santiago de Cuba (Cuba), *Communications Technology Group* (GTC), Aragón Institute of Engineering Research (I3A), University of Zaragoza (UZ) and CIBER - Bioingeniería, Biomateriales y Nanomedicina (BBN), Edificio I+D, C/ Mariano Esquillor S/N 50018 Zaragoza, Spain, (e-mail: {mnoriega, dromero}@unizar.es)

R. Almeida is with the CIBER - BBN, with the GTC, I3A, UZ, and with CMUP (e-mail: rbalmeid@unizar.es). J.P. Martínez, R. Bailón and P. Laguna are with the GTC, I3A, UZ, and with CIBER - BBN,(e-mail: {jpmart, rbailon, laguna}@unizar.es).

This work was partially supported by project TEC2007-68076-c02-02 from MCyT and FEDER, Grupo Consolidado GTC from DGA T:30, and grants from *Banco Santander Central Hispano* and UZ. CIBER-BBN is an initiative funded by the VI National R&D&i Plan 2008-2011, Iniciativa Ingenio 2010, Consolider Program, CIBER Actions and financed by the Instituto de Salud Carlos III with assistance from the European Regional Development Fund.*CMUP* is financed by *FCT*, Portugal, through the programmes POCTI and POCI 2010, with national and European Community Structural Funds.

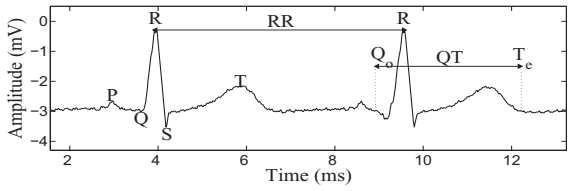

Fig. 1. Principal waves of a beat (P wave, Q, R and S waves (QRS complex) and T wave) and RR and QT intervals, corresponding respectively to the durations of the ventricular cycle and of the ventricular activity in each cycle. The R peak mark locate the beat and the marks of the beginning of QRS (Q_o) and of the T wave end (T_e) correspond respectively to the beginning and to the end of the ventricular depolarization and repolarization process.

Both ECG and VCG, frequently show physiological non cardiac contamination, such as mechanical respiratory effect. As a matter of fact the respiration not only induces changes in the length of the cardiac cycle (physiologic effect, by autonomic influence), but also in the waves' morphology as result of the thorax movement. The expansion and contraction of the lungs during the respiratory cycle change the heart electric axis and the impedance distribution on the thorax, resulting also in scaling and rotation on the ECG (Fig. 2). This

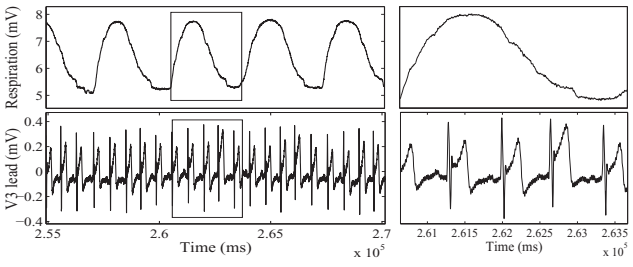

Fig. 2. Example of morphology changes of the ECG signal caused by respiration. On the right is a zoom of the area inside the rectangle.

is likely to cause errors in the T wave delineation as it typically presents a morphology of small amplitude and low signal to noise ratio (SNR). In a preliminary study, [3], we found that using a multilead delineation (ML) allows to increase the stability of the T wave end (T_e) location, with respect to using single -lead delineation (SL) or post processing rules after SL delineation (SLR). We hypothesize that this is a consequence of a lower influence of the mechanical respiratory effect over ML based automatic locations. To validate this hypothesis, in this work we performed a simulation study in which the

respiratory effect was controlled and the correct delineation of T_e is discussed. In particular, we also investigate in real signals whether the well-known mechanical influence of respiratory activity on the ECG is the same on the several strategies or affects the stability of the obtained marks.

II. Automatic Delineation

There are several published methodologies for automatic ECG delineation. Particularly in this work we use the multi-scale wavelet-based delineator previously described and validated in [4] and [5] that has shown to provide adequate boundaries locations.

A. SL and SLR for multilead signals

For each lead, a set of differentiated signals, smoothed at different scales, is obtained by means of the discrete wavelet transform (WT), using a quadratic spline wavelet. First, detection and classification of waveforms are performed by searching for the maxima and minima at different scales. Then, the waveform boundaries are located using a threshold approach across scales. This allows to obtain a set of annotations for each available lead [4]. The main limitation of this method is that the ECG waves are global phenomena and therefore is desirable to consider an approach in which all leads are taken into account to produce global marks.

One strategy for dealing with multilead signals is the inclusion of SLR after the SL based delineation. A simple rule is to choose the median of the SL marks as the peak of the wave. The mark for a wave's begin (end) should be the earlies (latest) one, with some outliers protection [6].

B. ML delineation

Although the SLR strategy finally gives one single mark per boundary or peak, it does not use all available spatial information. The ML delineation departs from the SL but considers simultaneously the orthogonal leads of the VCG [5]. Denoting the WT of a signal $s(n) \in \{x(n), y(n), z(n)\}$ in the WT scale m by $w_{s,m}[n]$, the spatial WT loop is defined as:

$$\mathbf{w}_m(n) = [w_{x,m}(n), w_{y,m}(n), w_{z,m}(n)]^T \quad (1)$$

As a consequence of the WT prototype smoothed used, the WT loop $\mathbf{w}_m(n) \,|n \in L$ is proportional to the VCG derivative and describes the velocity of evolution of the EHV in a time interval L. Assuming that the noise is spatially homogeneous, the direction with maximum projection of the WT in the region close to the wave boundary would define the ECG lead maximizing the local SNR, and thus, the most appropriate for boundary delineation. The main direction $\mathbf{u} = [\mathrm{u}_x, \mathrm{u}_y, \mathrm{u}_z]^T$ of EHV variations on any time interval L is given by the director vector of the best straight linear fit to all points in the WT loop. By choosing adequately the time interval L, around the fiducial point of interest, it is possible to find the direction $\mathbf{u}$ corresponding to the lead most suited for delineation purposes. The projection of the WT loop $(\mathbf{w}_m(n))$ over the direction $\mathbf{u}$ allows to obtain a derived wavelet signal $w_{d,m}(n)$ that combines the information provided by the 3 VCG leads:

$$w_{d,m}(n) = \frac{\mathbf{w}_m^T(n) \cdot \mathbf{u}}{\|\mathbf{u}\|};\ n \in I \quad (2)$$

It should be noticed that the time intervals I (used for projecting) and L (used for linear fitting) can be different, depending on each wave specificities.

The strategy proposed for ML boundary delineation using WT loops is based in a multi-step iterative search for a better spatial lead (with *steeper* slopes) for each boundary delineation. The goal is to construct a *derived wavelet* signal well suited for boundaries location, using the same detection criteria as in the SL delineator [5].

III. Materials and methods

A. Simulation study

1) Clean ECG simulation: An artificial 3-lead ECG signal $[x_c(n), y_c(n), z_c(n)]^T$ was constructed by concatenation of a scaled versions of a real template beat sampled at 500 Hz, following $RR(i)$ and $QT(i)$ series extracted from a PTB database [7] real file, where *i* is the beat number. The template beat (without apparent noise), was chosen from a 12-lead ECG, and the Frank leads were synthesized using *Dower* transformation [8]. SL delineation of the template beat was used to obtain the locations of the R peak, the QRS complex onset/end and the T_e. The reference mark for the R peak was taken from the 3 SL marks as the one corresponding to the largest signal amplitude, while for the boundaries were taken the earliest/latest marks for the onset/end.

To reflect the variability inherent to the correspondent clean series $QT(i)$, the template beat was properly scaled from the QRS end to the T_e reference mark, to produce the target QT interval. By applying the same scaling to each orthogonal lead, an artificial 3-lead ECG signal with the same variability in all leads and known T_e locations ($T_e^{\text{ref}}(i)$) is obtained [9].

2) Respiration effect: The mechanical effect of respiration was simulated over the artificial ECG as a cardiac electrical axis rotation [10]. For the sake of simplicity, the rotation was arbitrarily considered around the z axis, with a maximum angle of 15º (affecting only the leads $x(n)$ and $y(n)$).

The signals affected by respiration $[x_r(n),\ y_r(n),\ z_r(n)]^T$ were constructed from $[x_c(n),\ y_c(n),\ z_c(n)]^T$, by introducing the equivalent effect to a respiration given by a pure sinusoid $r(n)$ at a frequency $F_r \in \{0.15, 0.19, 0.24, 0.27, 0.40\}\ Hz$.

3) Noise contamination: Noise contamination was considered, by adding resampled pre-recorded noise $[x_v(n), y_v(n), z_v(n)]^T$ corresponding to residue at the initial stage of a real ECG stress test [11]. The noise was added to the ECG signal with respiratory effect ($F_r = 0.27\ Hz$ which corresponds to real respiratory signal frequency present in the *QT(i)* and *RR(i)* series used to construct the simulated signal). The 3 noise lead were rescaled by a constant a to get a SNR $\in \{30, 25, 20, 15, 10\}\ dB$:

$$a = \left(\frac{P_{x_r} + P_{y_r} + P_{z_r}}{P_{x_v} + P_{y_v} + P_{z_v}} \cdot 10^{\frac{-\text{SNR}}{10}} \right)^{1/2} \quad (3)$$

were P_s denote the power of signal $s(n)$.

4) Performance indexes: These simulated ECG signals (clean, with mechanical respiratory effect and with other added noise) were delineated with SL, SLR and ML to obtain, respectively, the marks T_e^{M}, $M \in \{\text{SL, SLR, ML}\}$. For SLR delineation first was applied the Dower's transformation to obtain the 12 standard leads [8].

To study the influences of the respiration on T_e delineation over the simulated ECG, the error in T_e mark was defined as:

$$\mathcal{E}_{\mathrm{M}}^{r}(i) = T_e^{\mathrm{M}}(i) - T_e^{\mathrm{ref}}(i);\ \mathrm{M} \in \{\text{SL, SLR, ML}\} \qquad (4)$$

The errors considering noise contamination ($\mathcal{E}_M^v$) were similarly calculated.

To evaluate the relation between the respiratory signal ($r(n)$) and the direction **u**, in both the clean ECG and with added noise respectively, the angles of **u** with respect to the plane defined by each pair of orthogonal leads ($\angle_P^r$ and $\angle v_P$; $P \in \{(x,y),(y,z),(x,z)\}$) were obtained.

The linear relation between the $r(n)$ and the series of $T_e(i)$ errors and the angles were measured using spectral coherence after resampling at 500 Hz. The average value of the spectral coherence in a *0.04 Hz* bandwidth centered on F_r was taken and denoted as $C_{r,\mathcal{E}_M^r}$ for the $\mathcal{E}_M^r$ and $C_{r,\angle_P^r}$ for the $\angle_P^r$. The average value of the spectral coherence considering noise contamination were similarly calculated to $\mathcal{E}_M^v$ and $\angle_P^v$.

B. Real ECG study

1) Data: To extend the study to real signals we used the 70 control records of PTB database [7]. Each record contains the 12 standard and the 3 Frank leads, sampled at 1000 Hz.

The ECG signals were delineated using the SLR and ML delineation strategies. The ML strategy was applied over Frank leads and SLR over the 12 standard leads; RT_e^M interval was measured from the R peak obtained with SLR to $T_e(i)$ for each delineation system $M \in \{\text{SLR, ML}\}$. The mechanical effect off respiration was extracted from the ECG signal using the algorithm proposed in [12]. In this method the ECG-derived respiratory signal is defined on each VCG lead by the series of least-squares rotation angles, $\varphi_x(i), \varphi_y(i)$ and $\varphi_z(i)$, estimated between successive QRS-VCG loops and some reference QRS-VCG loop.

2) Performance indexes: The delineation error over the real ECG signal can not be calculated as there is no reference T_e mark. Instead, the differences between the automatic T_e locations obtained using the two strategies were calculated:

$$\Delta T_e(i) = T_e^{\mathrm{SLR}}(i) - T_e^{\mathrm{ML}}(i) \qquad (5)$$

For the ML strategy we also obtained the angles of the direction **u** with respect to the plane defined by each pair of orthogonal leads ($\angle_P$; $P \in \{(y,z),(x,z),(x,y)\}$). As in the simulated data study, the linear relation between the $\varphi_l(i), l \in \{x,\ y,\ z\}$ and ΔT_e ($C_{r,\Delta T_e}$), RT_e^{M} ($C_{r,RT_e^{\mathrm{M}}}$) or $\angle_P$ ($C_{r,\angle_P}$) resampled at 500 Hz were measured using spectral coherence, taking the mean value in a *0.04 Hz* bandwidth centered on the estimated F_r.

IV. Results and Discussion

A. Simulation study

Figure 3 show the $r(n)$ and the time series of errors committed and the error $\mathcal{E}_M^r(i)$ for each delineation strategy. The relation between the errors obtained using SL and SLR with $r(n)$ is quite remarkable, while using ML it is not visible.

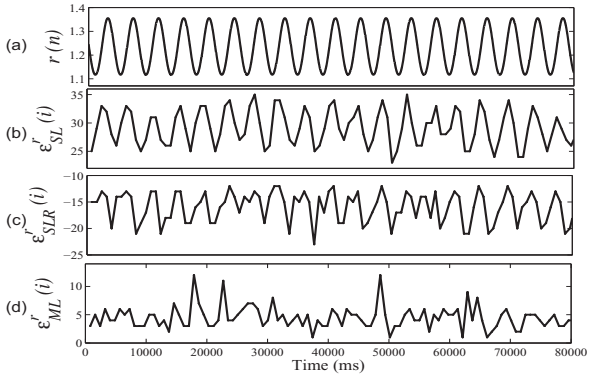

Fig. 3. Plot of simulated series, (a) respiratory signal (A.U.), (b), (c) and (d) errors $\mathcal{E}_M^r(i)$, (ms).

Table I presents the values of $\mathcal{E}_M^r(i)$ (mean $\pm$ standard deviation) for each studied F_r. The ML allows to reduce both the bias and the dispersion of the delineation error for all F_r values with respect to the SL and SLR delineators.

TABLE I
MEAN VALUES AND SD OF $\mathcal{E}_M^v(i)$ FOR EACH STUDIED F_r VALUE

F_r (Hz)	$\mathcal{E}_{\mathrm{SL}}^r$ (ms)	$\mathcal{E}_{\mathrm{SLR}}^r$ (ms)	$\mathcal{E}_{\mathrm{ML}}^r$ (ms)
0.15	29.3 ± 3.2	14.8 ± 1.9	4.4 ± 1.8
0.19	29.2 ± 3.4	14.8 ± 2.1	4.4 ± 1.6
0.24	29.3 ± 3.3	14.7 ± 2.1	4.3 ± 1.6
0.27	29.3 ± 3.3	14.8 ± 1.9	4.4 ± 1.8
0.40	29.3 ± 3.2	14.8 ± 2.0	4.4 ± 1.8

The main hypothesis to justify this lower influence of respiration on the ML marks is that the direction **u** adapts to respiration-induced changes in the EHV.

Figure 4 (a) shows the average coherence values ($C_{r,\mathcal{E}_{\mathrm{M}}^r}$). Note that the $C_{r,\mathcal{E}_{\mathrm{M}}^r}$ obtained with ML are lower than those obtained with SL and SLR for all studied F_r. This indicates that the marks T_e errors in ML delineation are less related to the mechanical effect of respiration. The Fig. 4 (c) show the $C_{r,\angle_P^r}$, and both the $\angle_{(x,z)}^r$ and $\angle_{(y,z)}^r$ have high values of coherence with $r(n)$, indicating a strong linear relation with the mechanical effect of respiration and justifying the lesser influence of the respiration on ML T_e mark. In the case of $C_{r,\angle_{(x,y)}^r}$ the values are lower because the cardiac electrical vector rotation was performed about this axis. The mean and SD values of $\mathcal{E}_{\mathrm{M}}^v$ are shown in the Table II. Again lower mean errors and SD are obtained with ML delineation. The $C_{r,\mathcal{E}_M^v}$ values indicate the lower influence of respiration on T_e mark in the presence of non-respiratory noise (Fig. 4 (b)). The coherence $C_{r,\angle_P^r}$ in the presence of noise (Fig. 4 (d)) is also slightly lower that in (Fig. 4 (c)).

B. Real ECG study

The distribution across records of the mean coherence values between the estimated $\varphi_x(i)$ and $RT_e^{\mathrm{M}}(i)$ or $\Delta T_e(i)$

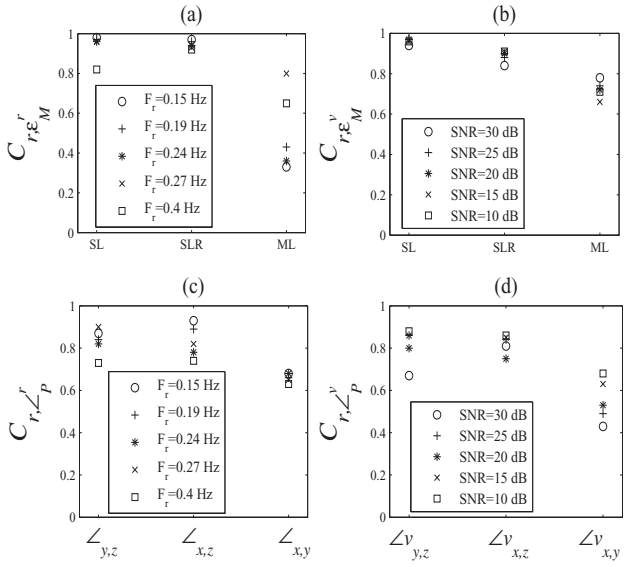

Fig. 4. Average coherence values of (a) $\mathcal{E}^r_M(n)$, (b)$\mathcal{E}^v_M(n)$, (c) $\angle^r_P(n)$ and (d) $\angle^v_P(n)$ series with $r(n)$.

TABLE II
MEAN VALUES AND SD OF $\mathcal{E}^v_M(i)$ FOR EACH STUDIED SNR VALUE

SNR (dB)	$\mathcal{E}^v_{\text{SL}}$ (ms)	$\mathcal{E}^v_{\text{SLR}}$ (ms)	$\mathcal{E}^v_{\text{ML}}$ (ms)
30	29.3 ± 3.1	14.9 ± 1.8	4.3 ± 1.7
25	29.9 ± 3.3	15.8 ± 1.9	4.8 ± 1.8
20	30.3 ± 3.2	15.9 ± 2.0	5.0 ± 1.9
15	30.2 ± 3.3	15.8 ± 2.3	5.2 ± 1.8
10	31.4 ± 3.5	16.3 ± 2.6	5.9 ± 2.3

are shown in Fig. 5 (a). $\Delta T_e(i)$ typically presents a strong relation with the $\varphi_x(i)$, indicating that most of the differences between the locations provided by the two strategies correlate with the respiration. This results indicate that the $RT^{\text{ML}}_e(i)$ series is less influenced by the respiration, with median of a coherence values of 0.59, below the value obtained in the $RT^{\text{SLR}}_e(i)$ series with median of 0.75. The results obtained with $\varphi_y(i)$ and $\varphi_z(i)$ are equivalent

The mean coherence values distribution between $\varphi_x(i)$ and

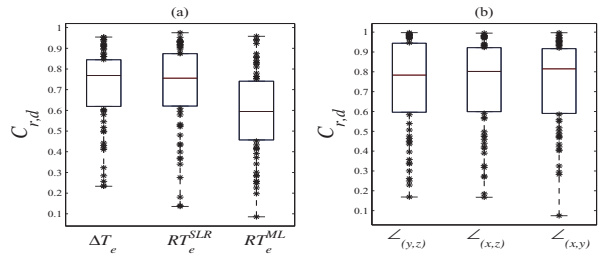

Fig. 5. (a) Average coherence values distribution with $\varphi_x(i)$ of $\Delta T_e(i)$, RT^{SLR}_e and RT^{ML}_e series. (b) Average coherence values distribution with $\varphi_x(i)$ of direction **u** angle series respect the (x, y), (x, z) and (y, z) planes.

the angles with respect to (y, z), (x, z) and (x, y) planes is shown in Fig. 5 (b). Note the strong relation between the direction **u** and the respiratory signal, this shows that the ML strategy is adapting the search for the best lead to mark T_e canceling out the morphologic effects caused by the respiration. Thus the lower coherence between the respiratory signal and RT^{ML}_e compared with RT^{SLR}_e, results from a lower influence from the mechanical effect of the respiration, confirmining the results obtained in simulation.

V. CONCLUSION

The results obtained in this study show the importance of multi-lead delineation. From comparison between the multi-lead strategies in both simulated and real signals, a lower influence of the mechanical effect of the respiration on the T_e mark location was observed with ML delineation. The differences between the T_e measures obtained with both ML and SLR, is dominated by respiratory mechanical influence on the SLR mark. In addition, we find out that the selected direction of projection **u** in the ML system follows the changes of the cardiac electrical axis caused by respiration, compensating their effect on the T_e mark. Thus the increased stability in the T_e mark in ML system with respect to SLR one can be explained by a reduction of the variability associated to the mechanical effect of respiration.

REFERENCES

[1] Sörnmo L, Laguna P. "Bioelectrical Signal Processing in Cardiac and Neurological Applications." Elsevier Academic Press, 2005.

[2] Malmivuo, J. and Plonsey, R. "Bioelectromagnetism - Principles and Applications of Bioelectric and Biomagnetic Fields." Oxford University Press, 1995.

[3] M. Noriega, R. Almeida, J.P. Martínez, P. Laguna. Medida Multiderivacional de QT en el ECG de 12 derivaciones del sistema EASI. XXVII Congreso Anual de la Sociedad Española de Ingeniería Biomédica (CASEIB 2009). Noviembre 18-20, 2009 Cádiz, España.

[4] Martínez JP, Almeida R, Olmos S, Rocha AP, Laguna P. "Wavelet-based ECG delineator: evaluation on standard databases." *IEEE Trans. Biomed. Eng.*, vol 51, 2004, pp 570-81.

[5] Almeida R, Martínez JP, Rocha AP, Laguna P. "Multilead ECG delineation using spatially projected leads from wavelet transform loops." *IEEE Trans. Biomed. Eng.*, vol 56, no 8, 2009, pp 1996-2005.

[6] Laguna P, Jané R, Caminal P. "Automatic detection of wave boundaries in multilead ECG signals: Validation with the CSE database." *Comput. Biomed. Res.*, vol 27, no 1, February 1994, pp 45-60.

[7] Christov, I., I. Otsinsky, I. Simova, R. Prokopova, E. Trendafilova and S. Naydenov, 2006. "Dataset of manually measured QT intervals in the electrocardiogram." *Biomedical Engineering Online* 31(5), 5-31.

[8] Dower GE. The ECGD: a derivation of the ECG from VCG leads. *Journal of Electrocardiol.*, vol 17, no 2, 1984, pp 189-91.

[9] Almeida R., J. P. Martínez, A. P. Rocha, S. Olmos and P. Laguna (2005) "Improved QT variability quantification by multilead automatic delineation." In: Computers in Cardiology 2005, Vol. 32 IEEE Computer Society Press, pp. 503-506.

[10] Aström, M., H. C. Santos, L. Sörnmo, P. Laguna and B. Wohlfart, 2000. "Vectorcardiographic loop alignment and the measurement of morphologic beat-to-beat variability in noisy signals." *IEEE Trans. Biomed. Eng.* 47(4), 497-506.

[11] R. Bailón, J. Mateo, S. Olmos, P. Serrano, J. García, A. del Río, I. Ferreira, and P. Laguna. "Coronary artery disease diagnosis based on exercise electrocardiogram indexes from repolarisation, depolarisation and heart rate variability." *Med. Biol. Eng. Comput.*, vol. 41, pp. 561-571, 2003.

[12] Bailón, R, L. Sörnmo and P. Laguna, 2006. "A robust method for ECG-based estimation of the respiratory frequency during stress testing." *IEEE Trans. Biomed. Eng.* 53, 1273-1285.